Science of the Total Environment 896 (2023) 165221

Contents lists available at ScienceDirect

Science of the Total Environment

journal homepage: www.elsevier.com/locate/scitotenv

Comparison of two 2-D numerical models for snow avalanche simulation

Marco Martini *, Tommaso Baggio, Vincenzo D'Agostino

Department of Land, Environment, Agriculture and Forestry, University of Padova, via dell'Università 16, 35020 Legnaro, PD, Italy

HIGHLIGHTS

- Calibration of numerical models to predict snow avalanche dynamics
- Performances of RAMMS and FLO-2D models are assessed by means of statistical indices.
- Hydraulic model FLO-2D could be a valid support for snow avalanche hazard mapping.

GRAPHICAL ABSTRACT

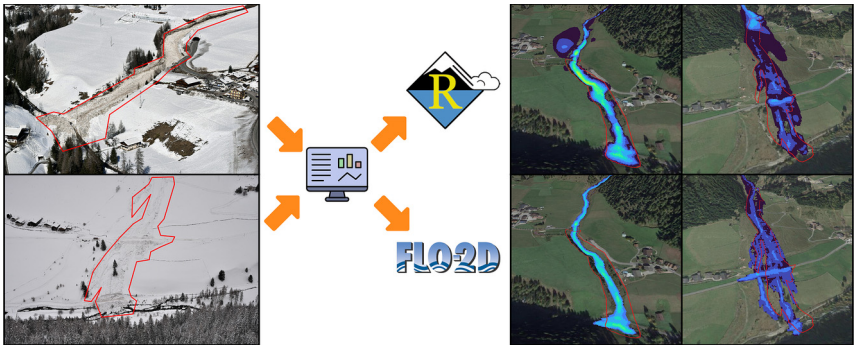

ARTICLE INFO

Editor: Ouyang Wei

Keywords:
Snow avalanche
Dynamic modelling
Back analysis
Hazard mapping

ABSTRACT

Snow avalanches are gravitational processes characterised by the rapid movement of a snow mass, threatening inhabitants and damaging infrastructure in mountain areas. Such phenomena are complex events, and for this reason, different numerical models have been developed to reproduce their dynamics over a given topography. In this study, we focus on the two-dimensional numerical simulation tools RAMMS::AVALANCHE and FLO-2D, aiming to compare their performance in predicting the deposition area of snow avalanches. We also aim to assess the employment of the FLO-2D simulation model, normally used in water flood or mud/debris flow simulations, in predicting the motion of snow avalanches. For this purpose, two well-documented avalanche events that occurred in the Province of Bolzano (IT) were analyzed (Knollgraben, Pichler Erschbaum avalanches). The deposition area of each case study was simulated with both models through back-analysis processes. The simulation results were evaluated primarily by comparing the simulated deposition area with the observed one through statistical indices. Subsequently, the maximum flow depth, velocity and deposition depth were also compared between the simulation results. The results showed that RAMMS::AVALANCHE generally reproduced the observed deposits better compared to FLO-2D simulation. FLO-2D provided suitable results for wet and dry snow avalanches after a meticulous calibration of the rheological parameters, since they are not those typically considered in avalanche rheology studies. The results showed that FLO-2D can be used to study the propagation of snow avalanches and could also be adopted by practitioners to define hazard areas, expanding its field of application.

1. Introduction

Snow avalanches are typical natural hazards of mountain areas that constitute serious threats to infrastructure (buildings, roads, and bridges) and, above all, to the local inhabitants and visitors (McClung and Schaerer, 2006). During the 30 years 1991–2020, the average number of deaths caused by snow avalanches in the alpine region (including the French Pyrenees and Italian Apennines) was 95 per year, while there were 111 victims during the winter season of 2021 (Valt and Cianfarra, 2021). To deal with snow avalanche hazards, effective risk management is of great importance to increase the safety of residents and infrastructure. Snow avalanches are

* Corresponding author.
E-mail address: marco.martini.9@phd.unipd.it (M. Martini).

http://dx.doi.org/10.1016/j.scitotenv.2023.165221
Received 24 March 2023; Received in revised form 19 May 2023; Accepted 28 June 2023
Available online 29 June 2023

extremely complex gravity-driven phenomena characterised by the rapid movement of a snow mass with a volume >100 m^3 along a slope for a distance of at least 50 m (Rudolf-Miklau et al., 2015). Their motion involves aspects of fluid, particle and soil mechanics (Harbitz et al., 1998). Thus, the physical processes responsible for the formation of these phenomena, as well as their flowing mechanisms, have been studied since the late 19th century (Ancey, 2008; Harbitz et al., 1998; Rudolf-Miklau et al., 2015; Salm, 2004; Schweizer et al., 2003). The complexity of snow avalanches once in motion can be approximated with simplified models based on physical and mathematical physics (Rudolf-Miklau et al., 2015). Despite that, a full physically based description of snow avalanche dynamics does not yet exist due to the large variability of the snow material and the limited understanding of the flowing dynamics (Ancey, 2008; Naaim et al., 2013; Rudolf-Miklau et al., 2015).

Eckert and Giacona (2023) distinguish snow avalanche risk into short-term and long-term risks. The former mainly involves recreational activities (such as skiing) and is systematically managed through weather and snow condition forecasts. The second concerns the threat to infrastructures and human lives in settlements in risk zones. In this paper, we focus on the concept of risk referring to long-term risk. Effective risk mitigation requires cautious land-use planning, through the definition of hazard maps that represent the base for risk analysis and successively for the implementation of a defence structure. The practices and policies of snow avalanche risk management vary among countries (and sometimes from region to region). However, some common aspects are hazard, vulnerabilities and risk assessment and mapping, land-use planning, design of mitigation measures, risk management and resilience estimation (Eckert and Giacona, 2023). Frequently, the guidelines regulating and defining snow avalanche hazard mapping require the use of numerical modelling/simulation tools (e.g. Civil Protection Agency of the autonomous province of Bolzano–Bozen - Provincial Functional Centre, 2017). Dynamic numerical models are employed to predict the possible areas affected by snow avalanche events and then derive hazard maps through the combination of different scenarios. Therefore, numerical models play a crucial role in land-use planning, and for this purpose, they should reliably represent the characteristics of future snow avalanches.

The need to improve the reliability of snow avalanche predictions in terms of run-out distance, flow velocities, impact pressures and the spread of deposits on natural three–dimensional terrain led to the development of several snow avalanche models characterised by different approaches. Harbitz et al. (1998) provided a complete review of snow avalanche models, which were then analyzed and expanded by other authors (e.g., Ancey, 2008; Barbolini et al., 2000; Jamieson et al., 2008; Rudolf-Miklau et al., 2015; Salm, 2004). Avalanche models can be divided into two types: (1) empirical procedures based on statistical–topographical models (Eckert et al., 2008; Eckert et al., 2007; Lied and Bakkehoi, 1981; McClung, 2001; Meunier and Ancey, 2004); (2) physical-dynamic models based on a fluid–mechanic approach with different degrees of complexity (Salm, 1993; Salm et al., 1990; Savage and Hutter, 1991; Savage and Hutter, 1989; Voellmy, 1955). Statistical–topographical models are often site-specific methods that, through regressions or distribution parameters derived from a dataset of observed events, can be used to calculate the probable run-out distance of future snow avalanches (Jamieson et al., 2008). Widely adopted statistical models are the so-called Alpha–Beta models (Lied and Bakkehoi, 1981). Physical–dynamic models are based on physical laws, such as mass and momentum conservations, to estimate the run-out distance and velocity of the centre of mass or the front of the avalanche over a simplified representation of the topography. Ancey (2008) divided physical–dynamic models into simple models, such as the widespread Voellmy – Salm – Gubler (VSG) model (Salm, 1993; Salm et al., 1990; Voellmy, 1955), and intermediate models, which use depth-averaged mass and momentum equations, such as, for example, the model proposed by Savage and Hutter (1989, 1991). Generally, physical–dynamic models are developed specifically to reproduce the behaviour of one type of avalanche flow (i.e., dense or powder flow). Most models are developed for dense flow avalanches, whereas only a few can simulate powder flow avalanches or both (Sampl and Zwinger, 2004). Voellmy (1955) described dense flow avalanche motions mathematically by treating the sliding mass as a continuum fluid subject to a velocity-squared-dependent turbulent friction term (ξ), similar to the Chezy resistance for turbulent water flow in open channels, and a basal Coulomb-like dry friction term (μ). Subsequent works (see, e.g., Perla et al., 1980; Salm, 1966; Savage and Hutter, 1989, 1991) further developed the Voellmy model, realising mathematically similar one-dimensional mass-centre models (Barbolini et al., 2000; Salm, 2004). The most widely adopted modified form of the Voellmy model is the Voellmy–Salm–Gubler model (Gubler, 1994; Salm, 1993; Salm et al., 1990), and requires few computational resources, representing avalanche motion as sliding blocks. Two-dimensional models are the most used in hazard mapping by practitioners, providing distribution of the flow depth and the associated mean flow velocity. In fact, these can be used, coupled with the flow material density (based on snow density values reported in the literature and/or derived from direct field or laboratory experiences), to estimate impact pressures along the path. Over the years, more complex and advanced physical–based models have been developed, with the aim of improving their reliability. Recently, more advanced snow avalanche routing models have been developed considering different physical processes associated with the granular characteristics of avalanches (Buser and Bartelt, 2009; Naaim et al., 2003) and snow entrainment and deposition phenomena (Christen et al., 2010b; Naaim et al., 2003; Sovilla et al., 2008; Sovilla et al., 2006). The rheology laws of these models are affected by uncertainties related to the values of the flow parameters associated with the flow resistance (Jamieson et al., 2008). The rheological parameters of simulation models can be obtained through back–calculation of well-documented events (Barbolini et al., 2000; Christen et al., 2010a; Gruber and Margreth, 2001; Jamieson et al., 2008; Maggioni et al., 2012; Sanz-Ramos et al., 2021). Thanks to the increase in computer performance, physical–based models have been implemented in simulation tools capable of predicting the propagation of a flow over a defined topography (by means of Digital Elevation Models – DEMs) starting from a release area. Examples of such simulation tools are the two-dimensional models RAMMS::AVALANCHE (Christen et al., 2010b), SamosAT (Sampl and Zwinger, 2004), r.avaflow (Mergili et al., 2017) and DAN-3D (Aaron et al., 2016). More recently, machine learning techniques applied to big data collections have been used to evaluate the susceptibility of occurrence (Blagovechshenskiy et al., 2023; Choubin et al., 2019; Liu et al., 2023), assess mass wasting susceptibility (Choubin et al., 2020), or runout distance (Toft et al., 2023) over large spatial extents.

Since snow avalanche simulation tools are used to prevent victims and damage to human activities, it is important to evaluate their overall performance and limits (Barbolini et al., 2000). At the moment, however, the number of widely used tools specifically developed for two-dimensional snow avalanche dynamic simulations is still limited. The availability of a flexible simulation tool that could reproduce phenomena for which it was not specifically developed can be of great help to practitioners to enlarge the options for simulating snow avalanches. FLO-2D (O'Brien et al., 1993) is one of the most widely used two–dimensional flow simulation tools developed to simulate flood and debris/mud flow. Although FLO-2D was developed for flood and debris/mud flow simulation, some examples of its use to simulate snow avalanches and risk mapping are reported in the literature (Barbolini and Savi, 2014; Moro, 2009). These studies are limited and are not sufficient to correctly assess their reliability in predicting snow avalanche motion. Since the rheological parameters in FLO-2D refer to those for debris flow, the need for adapted values in the case of model application to snow avalanches becomes a bottleneck for model extension, also considering the scarcity in the literature of such implementation and comparison between FLO–2D and other models. Therefore, evaluating the employment of FLO-2D in snow avalanche simulations, and comparing the performance of the model with a model specifically designed for this purpose could be of interest to practitioners as a practical support for hazard mapping (Barbolini and Savi, 2014). Moreover, the model comparison could be a valuable indication to better assess the model performance and to widen the hazard scenarios accounting for different modelling hypotheses.

There are only few recent studies in the literature where two-dimensional simulation tools are compared. Schmidtner et al. (2018) compared RAMMS::AVALANCHE and SamosAT by simulating three documented snow avalanches. Their results show that RAMMS::AVALANCHE simulated slightly higher maximum velocities (above 25 m/s) and longer runout than SamosAT in all the case studies, while the latter simulates larger lateral extension. Zugliani and Rosatti (2021) used RAMMS::AVALANCHE to validate their newly developed two-dimensional model TRENT2D*.

The objective of this study is to test the performance of the two-dimensional model FLO-2D in simulating snow avalanche dynamics and compare its results with the two-dimensional avalanche dynamic simulation tool RAMMS::AVALANCHE (Christen et al., 2010b). Since RAMMS::AVALANCHE is one of the most widely used two-dimensional snow avalanche simulation tools and has been successfully applied in the Alps (Christen et al., 2010a; Dreier et al., 2016), Carpathians (Košová et al., 2022), Pyrenees (Riba Porras et al., 2018), Himalayas (Bartelt et al., 2016; Singh et al., 2020), and in the Andes (Janeras et al., 2013), it represents a good reference to evaluate the performances of FLO-2D. Furthermore, considering the uncertainties in the estimation of snow avalanche flow velocity (Fischer et al., 2014; Gauer, 2014), this investigation could help in the drawing up of composite hazard maps resulting from merged numerical modelling. To achieve this goal, we back-calculated two well-documented dense snow avalanches observed in the autonomous province of Bolzano–Bozen (South Tyrol, Italy), with the aim of highlighting the benefits and drawbacks of each model and the similarities and differences between them. After a presentation of the case studies, the main features of the two models are outlined focusing on the respective rheological laws, which regulate energy dissipation in motion. Then, result comparison - in terms of model performance of the back-analysis conducted - brings to the final discussion. The latter, learning from the response obtained from an accurate model calibration, aims to address the use and interpretation of the two models and the results obtained.

2. Study areas and snow avalanche events

The snow avalanche events studied in this work took place in the autonomous province of Bolzano–Bozen (South Tyrol) in the eastern Italian Alps (Fig. 1). This region extends over approximately 7400 km^2 with a typical mountain morphology. The elevation ranges from 3905 m a.s.l. of the Ortler in the western part of the region, to about 200 m a.s.l. at the valley bottoms located in the southern part. Generally, the south-eastern part of the area is characterised by the lower elevations (usually below 3000 m a.s.l.) and belongs to the Dolomites. These are sedimentary rock formations with rolling morphology interrupted by sharp cliffs. The formations located in the remaining part of the region have higher elevations with steeper valley sides and are composed of metamorphic and igneous rocks. South Tyrol has a relatively dry climate, with annual precipitation ranging from 500 mm to 1500 mm. Stable snow cover during winter months (>150 days/year) has been observed in the last decades only above elevations of 1200 m a.s.l. or higher (Adler et al., 2015; Pistocchi and Notarnicola, 2013). The first event, the Knollgraben avalanche, occurred on 10/03/2014 in the basin of the Rio Lappago-Knollbach, in the Valle dei Molini-Mühlwalder Tal. The second event, the Pichler Erschbaum avalanche, occurred on 02/02/2019 in the basin of Rio di Monterosso-Rotenbergbach, in the Pennes-Penser Valley. The events were documented by the Avalanche Cadastre of the Civil Protection Agency of the autonomous province of Bolzano–Bozen during post-event surveys. Both events were spontaneously triggered slab avalanches, however, they differed in their rheological characteristics. In this way, we can test the ability of FLO-2D and RAMMS::AVALANCHE to simulate different types of flow.

2.1. The avalanche event "Knollgraben"

The avalanche occurred on 10 March 2014, during the afternoon (between 12 p.m. and 6 p.m.), at the Knollgraben site. This slope is located

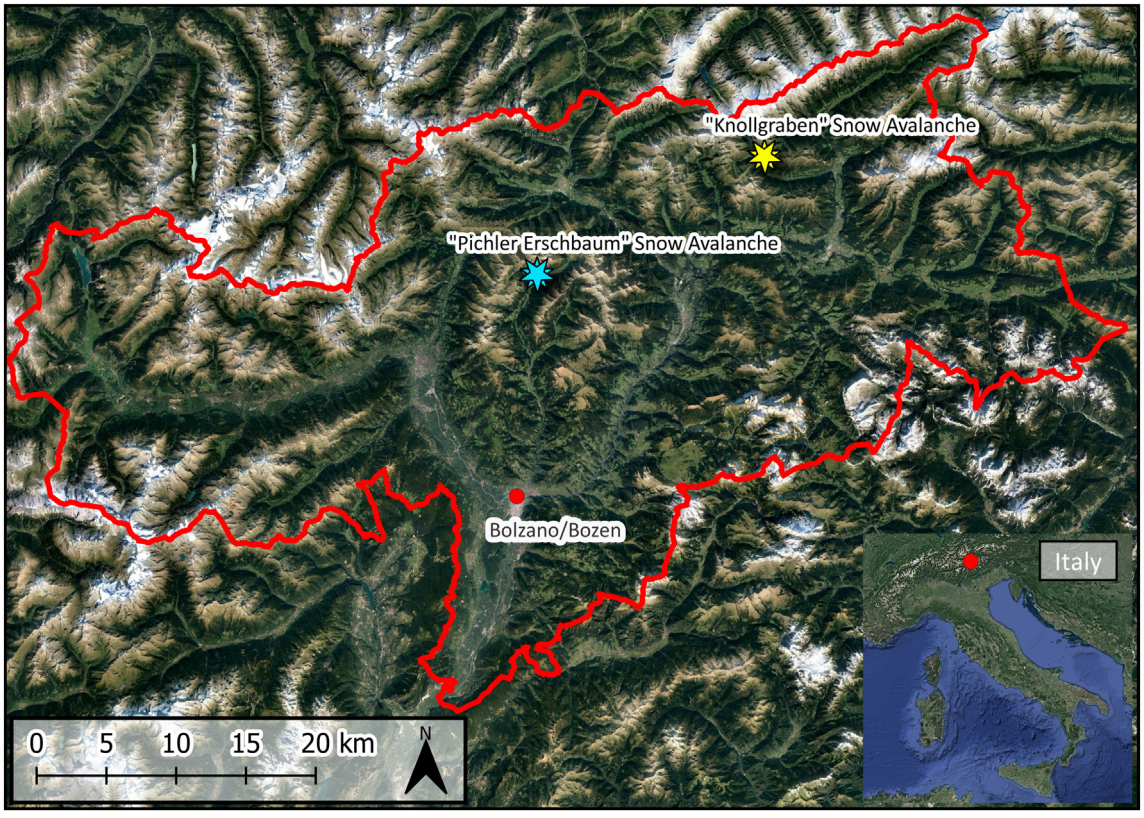

Fig. 1. Aerial overview of the autonomous province of Bolzano/Bozen and locations of snow avalanche sites (yellow: "Knollgraben" snow avalanche site; blue: "Pichler Erschbaum" snow avalanche site).

within the Rio Lappago-Knollbachn catchment near the town of Selva dei Molini-Mühlwald. The Rio Lappago-Knollbach catchment ranges from 2479 m a.s.l. of the mountain ridge to 1323 m a.s.l. at the confluence with the Rio Selva dei Molini-Mühlwalderbach. The catchment extends from north–east towards south–west and the mean slope is 36°. The alluvial fan of the catchment is located between an altitude of 1475 m a.s.l. and the confluence with the Rio Selva dei Molini-Mühlwalderbach and has a mean slope of 16.5°. The basin is formed by two small catchments that merge in one channel at 1670 m a.s.l. The Knollgraben avalanche site is characterised by the presence of a mixed forest of Norway spruce (*Picea abies*) and silver fir (*Abies alba*), with European larch (*Larix decidua*) in the upslope part. The forest cover surrounds the channel of the Rio Lappago-Knollbach. However, the trees do not cover the channel banks and the area affected by the avalanche. The vegetation in the release area is sparse, and the soil is covered by a grassland or meadow with rocky outcrops without forest cover. In the depositional area, the channel is surrounded by grassland or meadows, and the channel banks are covered by trees. The geology of the area is characterised by the presence of calc schists with ophiolites. On the three days preceding, as well as on the day of the event, the weather was warm (the mean maximum temperature for the four days was 8.3 °C at an elevation of 1470 m a.s.l.), and no precipitation was recorded in the study area. The position and dimensions of the release area were reconstructed using photographic material collected during the post-event survey on 11 March 2014. Detachment of the snow masses was considered spontaneous. The release area was identified thanks to post–event photographs of the slope on the hydrographic left side of the Rio Lappago-Knollbach at an altitude between 2418 m a.s.l. and 2132 m a.s.l. The detached snowpack covered a surface of 44,000 m^2. The mean slope of the release area was 36°. The mean snowpack height in the release area recorded on the day of the event was 200 cm, and the snow was described as "wet". The detached snow mass had a depth of 150 cm, and the estimated detached volume was about 66,000 m^3. The avalanche was characterised as a dense flow. The snow avalanche flowed along the channel of the Rio Lappago-Knollbach and stopped inside the talweg of the channel of the Rio Selva dei Molini-Mühlwalderbach (Fig. 2). During the post–event survey, a maximum depth of 8 m and maximum width of 70 m of the deposit were measured.

2.2. The avalanche event "Pichler Erschbaum"

The snow avalanche occurred early in the morning on February 2019, around 5.30 am at the Pichler Erschbaum site. This slope is part of the Rio di Monterosso-Rotenbergbach catchment, a small basin near the village of Rio Bianco–Weißenbach. The catchment ranges from 2277 m a.s.l. of the ridgeline to 1325 m a.s.l. at the confluence with the Talvera–Talfer River, extending from north towards south with a mean slope of 39°. The alluvial fan of the catchment is located between an altitude of 1525 m a.s.l. and the confluence with Talvera–Talfer River, and has a mean slope of 14.5°. At an elevation of 1366 m a.s.l., the Rio di Monterosso–Rotenbergbach flows under the national road SS 508. The Pichler Erschbaum avalanche site is characterised by the presence of a mixed forest of Norway spruce (*Picea abies*) and silver fir (*Abies alba*). The forest cover surrounds the channel of the Rio di Monterosso-Rotenbergbach. However, the trees do not cover the channel banks and the area affected by the avalanche. The vegetation in the upstream part of the headwater of the Rio di Monterosso-Rotenbergbach catchment is sparse, and the soil is covered by a grassland or meadow with rocky outcrops without forest cover, while in the downstream part, there are clusters of Norway spruce. However, these clusters do not cover the areas identified as probable release areas. In the depositional area, the channel is surrounded by pastures or meadows. The geology of the area is characterised by the presence of orthogneiss. Due to weather conditions at the time of the post-event survey (4 February 2019), it was not possible to accurately estimate the boundaries and position of the release area, nor the depth of the snowpack and of the release. However, due to data from previous events that occurred at the Pichler Erschbaum avalanche site and by studying the site topography (slope, exposition,

Fig. 2. Deposition of the "Knollgraben" snow avalanche event on 10 March 2014 (Selva dei Molini–Mühlwald, Autonomous Province of Bolzano – Bozen, Italy). Credits: Civil Protection Agency of the Autonomous Province of Bolzano – Bozen.

curvature) and the presence of vegetation, it was possible to define the location of the release areas. The first area ("Area 1") is located at an altitude between 2206 m a.s.l. and 1940 m a.s.l. and covers a surface of 22,338 m^2; the second area ("Area 2") has an extent of 16,949 m^2 and is located at an altitude between 2059 m a.s.l. and 1908 m a.s.l. The mean slopes of the release areas are 49° and 45° respectively. To define the depth of the snowpack, we used data available from the nearest meteorological station, located 7.5 km away (east-north direction) from the study area, at an altitude of 2127.5 m a.s.l. Data recorded by this station are also considered reliable for the Pichler Erschbaum avalanche site, since it is located in the same valley and at a similar altitude. At the time of the event (between 5 and 6 a.m.), the snow depth was 116 cm. On the two days before the event, the study area was affected by snowfall and the fresh snow accumulated during the last precipitation was equal to 53 cm. The snow was dry and the avalanche was characterised by a dense flow. The snow avalanche flowed down the gully of the Rio di Monterosso–Rotenbergbach until it reached the alluvial fan. The snow avalanche moved over it also spread outside the channel. Halfway up the alluvial fan, the snow mass divided into two branches. Most of the mass continued along the main flow direction, crossed the state road SS 508, and flowed downslope until it reached the Talvera–Talver River where it stopped (Fig. 3). Only a limited part of the snow mass continued to flow inside the channel of the Rio di Monterosso-Rotenbergbach and then stopped near the SS 508 road. The geospatial data collected after the event report an estimated maximum depth and maximum width of the main deposit of 5 m, and 73 m respectively.

3. Materials and methods

To compare the performance of the simulation tools RAMMS::AVALANCHE and FLO–2D in the back-calculation of observed snow avalanche events, we performed numerous simulations of the previously described events. The results obtained from the two simulation tools are first evaluated with (1) data collected by the Civil Protection Agency of the Autonomous Province of Bolzano–Bozen (Italy) during post–event surveys, (2) data reported in the scientific literature, and (3) by means of two statistical indexes. Then the simulation results of RAMMS::AVALANCHE and FLO–2D are compared to assess similarities and differences. In the following sections, a brief description of the two simulation tools is presented, followed by an overview of the geospatial data employed in the simulations. Thereafter, the input parameters of the two simulation tools are reported for the two avalanche events. Finally, the evaluation and validation criteria for the simulation results are explained.

3.1. The simulation tool FLO-2D

FLO-2D (O'Brien et al., 1993) is a finite volume conservation flood routing model, developed by "FLO–2D Software, Inc.". The tool simulates the propagation of flows on a given topography, defined by means of Digital Elevation Models (DEMs). The flood propagation is controlled by the resistance of the flow to the motion on a series of tiles of the grid (overland flows) or along stream segments (channel routing). Two–dimensional flood routing is achieved through finite-difference integration of the motion equation and the conservation of fluid volume both for a liquid flood or a hyper-concentrated sediment flow. The motion equation implemented in FLO–2D includes the continuity equation and the momentum equation (full dynamic wave equation) (Eqs. (1) and (2)):

$$\frac{\partial h}{\partial t} + \frac{\partial hV}{\partial x} = i \tag{1}$$

$$S_f = S_0 - \frac{\partial h}{\partial x} - \frac{V}{g} - \frac{\partial V}{\partial x} - \frac{1}{g} - \frac{\partial V}{\partial t} \tag{2}$$

where h is the flow depth, g is the gravitational accelleration and V is the depth-averaged velocity in one of the eight possible directions x and i is the excess rainfall intensity (could be non–zero on the flow surface). S_f is

Fig. 3. Deposition of the "Pichler Erschbaum" snow avalanche event of February 2019 (Sarentino–Sarnthein, Autonomous Province of Bolzano- Bozen, Italy). Credits: Civil Protection Agency of the Autonomous Province of Bolzano–Bozen.

the friction slope component and is based on Manning's equation. Other terms include the slope of the bed (S_o), the terms of pressure gradient, and the convective and local acceleration. The equation represents the one-dimensional depth-average channel flow. Although FLO-2D is a multi-directional flow model, its motion equations are used by defining the average flow velocity across a grid element boundary in one direction at the time among the eight possible directions.

FLO-2D (MUDFLOW module) can also route hyper-concentrated flows such as mudflows and debris flows as fluids continuum. Viscous fluid motion is predicted as a function of the sediment concentration (C_v). To achieve sediment continuity, the tool employs a quadratic rheologic model to predict viscous and yield stresses. As a response to C_v changes for a given grid element, FLO-2D simulates dilution effects, mudflow cessation and deposit remobilization. The shear stress relationship used in FLO-2D is depth-integrated and rewritten as a dimensionless slope. The total friction slope (S_f) is composed of the sum of the yield slope, viscous slope and turbulent dispersive slope (Eq. (3)):

$$S_f = \frac{\tau_y}{\gamma_m h} + \frac{K\,\eta\,V}{8\,\gamma_m h^2} + \frac{n_{td}^2\,V^2}{h^{4/3}} \tag{3}$$

where γ_m is the specific weight of the sediment mixture, V is the depth-averaged flow velocity, K is the resistance parameter for laminar flow, n_{td} is the flow resistance of the turbulent-dispersive shear stress components (combined into an equivalent Manning's n-value for the flow), τ_y is the yield stress and η is the viscosity of the fluid. FLO–2D adopts a quadratic equation solution to the friction slope equation to apply it to the momentum equation. The viscous and turbulent-dispersive slope terms are written as depth–averaged velocity (V). Inflows and outflows are defined as flood hydrographs. It is possible to assign an input hydrograph to more than one element of the grid. In mud and debris flow simulations, a volumetric sediment concentration (C_v) or sediment volume must be defined for each water discharge.

3.2. The simulation tool RAMMS::AVALANCHE

RAMMS::AVALANCHE (Rapid Mass Movement Simulation) (Christen et al., 2010b) is a two–dimensional numerical simulation model developed by the WLS Institute for Snow and Avalanche Research SLF (Zurich, Switzerland) to calculate the motion of snow masses from the initiation area to the runout zone in three–dimensional terrain. The model uses depth-averaged equations to predict the flow heights and slope-parallel velocities of flows containing fast moving particles of snow surrounded by an interstitial fluid (air). The friction law is based on the Voellmy–Salm–Gubler (VSG) friction model, where the friction resistance is divided into: (1) a velocity-squared dependent turbulent friction term (ξ), similar to Chezy resistance for turbulent water flow in open channels, and (2) a Basal Coulomb-like dry friction term (μ) dependent on the internal shear angle of the snow material. In RAMMS::AVALANCHE the frictional parameters can be set as uniform or spatially variable within the computational domain. Alternatively, the tool automatically calculates friction values according to the topography (i.e. angle and curvature), altitude, and depending on the return period and magnitude of the avalanche (referred to as the "automatic method" in this work). In RAMMS::AVALANCHE the VSG model has been modified to consider the cohesion of the snow, expressed as yield stress (N_0), and the centrifugal forces derived from the terrain curvature, implemented inside the normal force term (N). The equation of the friction model used by RAMMS::AVALANCHE is:

$$S = \mu N + \frac{\rho g u^2}{\xi} + (1-\mu) N_0 e^{-\frac{N}{N_0}} \tag{4}$$

The input data for the simulations are defined by the practitioner and they are: (1) a Digital Elevation Model (DEM) as a representation of the topography; (2) the location and height of the released snowpack; (3) the rheological parameters density (ρ), cohesion (yield stress - N0) and friction parameters (μ and ξ).

3.3. Topographic and snow avalanche information

The back-calculation process required three different types of data: (1) the characterization of the initial conditions, (2) the representation of the basal topography (DEM) and (3) the post–event description of avalanche path and characteristics of the release and deposition areas. The initial condition data are the snowpack height, cumulated fresh snow, snow type (i.e., wet, dry, or loose snow) and the land use (to adequate the frictional parameters). These data are provided by the Snow Avalanche Cadastre of the Civil Protection Agency of the Autonomous Province of Bolzano–Bozen (Italy). The topography of the site is defined by means of Digital Terrain Models (DTM), freely available from the Geocatalog of the Autonomous Province of Bolzano–Bozen (Italy). DTMs have a spatial resolution of 2.5 m and were realised in 2006 from LiDAR data. Regarding the release areas, the information needed to set up the back analysis of the events are: the flowing mechanism of the snow avalanche (flowing avalanche or airborne avalanche), typology of release (slab or loose snow avalanche, surface-layer or full-depth avalanche), the snow depth of the released mass (full snowpack height in the case of full-depth avalanche), position, elevation, dimensions, and a georeferenced representation of the release area. Regarding the deposition area, the required post-event data are: the position, elevation, dimensions, and a georeferenced representation of the deposition area. To better evaluate the results of the back calculation, a georeferenced representation of the snow avalanche path is also needed. All these data are also provided by the Snow Avalanche Cadastre of the autonomous province of Bolzano–Bozen. Therefore, we compared the release and deposition areas of the observed and simulated avalanches and the results of the two simulation tools. Due to the lack of specific field data on snow density, we considered reference values suggested in the literature (Dent and Lang, 1982; McClung and Schaerer, 2006). Snow density (ρ) was set equal to 300 kg m^{-3} (setting γ_m = 3000 N m^{-3} in FLO-2D) for both case studies. For the Pichler Erschbaum snow avalanche, the depth of the detached snow was unknown. Therefore, we first considered a depth equal to the snow depth accumulated during the last precipitation (53 cm accumulated in the last two days before the event). However, using this value, it was not possible to correctly simulate the observed deposit. Hence, we consider a depth value equal to 100 cm.

3.4. FLO-2D simulations

Since there is no snow avalanche simulation module within FLO-2D, the flow resistance equation (Eq. (3)) was adapted to a form close to the Voellmy–Salm–Gubler (VGS) model by omitting the dynamic viscosity coefficient as proposed by Barbolini and Savi (2014) (Eq. (5)).

$$S_f = \frac{\tau_y}{\gamma_m h} + \frac{n_{td}^2\,V^2}{h^{4/3}} \tag{5}$$

where V is the depth averaged velocity, γ_m is the snow specific weight. τ_y (cohesive yield stress) and n (Manning's coefficient) are the friction parameters. By reducing the number of unknown coefficients, calibration of the model should thus be easier. The rheological low (Eq. (3)) was adapted to the simulation of a snow avalanche by setting the dynamic viscosity parameter (η) equal to η = 0 [Pa s]. The laminar flow resistance coefficient (K) was set equal to K = 2000 for all case studies. This was the mean value for the "spare vegetation class" proposed by Woolhiser (1975).

For each case study, multiple simulations were performed, testing different values of the rheological parameters by systematically and incrementally adjusting them to reproduce the occurred event as well as possible. For each event, the volume of the detached snow mass (Vol) was derived by multiplying the average depth of the detached snowpack by the surface of the release areas. The volumes of snow masses were then converted into inflow hydrographs represented by the water discharge (m^3 s^{-1}) and

sediment concentration (C_v) over time. To simulate the rapidity of the snow release, we considered hydrographs divided into 6-time steps of 1 s each and constant discharge values. Since the FLO-2D input hydrographs are associated with a single element of the grid, the previously calculated water discharge was then divided by the number of cells designated as inflow cells, and an inflow hydrograph assigned to each of them. With respect to *Cv*, different values of the parameter were tested to define how it affects the simulation results. Different values of cohesive yield stress (τ_y) were tested. Depending on the type of snow involved in each event, several reference values of snow cohesion reported in the scientific literature were considered (Bartelt et al., 2015; Dent and Lang, 1982; Joshi et al., 2006). Different values of Manning's *n* roughness coefficient (*n*–value) were tested, starting from the values proposed in (FLO-2D, 2019). All simulations were performed with a simulation time of 12 min (0.20 h). Table 1 reports the mass volume and the values or ranges of the rheological parameters considered in the FLO–2D simulations.

3.5. RAMMS::AVALANCHE simulations

For each case study, multiple simulations were performed, testing different values of the rheological parameters to reproduce the real event as well as possible. The volumes (*Vol*) of the detached snow masses were automatically computed by the tool from the release areas and the depth of the detached snowpack. Regarding frictional parameters (μ and ξ), we first performed a simulation with the values automatically defined by the software to test their reliability under different boundary conditions. For this purpose, the most realistic return period of the event (*Rp*) and the size class (*Size*) were defined as proposed by Christen et al. (2017) for each case study. However, it was not possible to correctly simulate the Pichler Erschbaum snow avalanche using the suggested values of the frictional parameters. Therefore, we tested different sets of μ and ξ in accordance with the topography of the run-out area. Different μ and ξ values were tested, both for the gully section and the alluvial fan, by systematically and incrementally adjusting them aiming to reproduce the occurred event as well as possible. Furthermore, different values of snow cohesion (yield stress N_0) were tested. Depending on the type of snow involved in each event, different reference values reported in the scientific literature were considered (Bartelt et al., 2015; Dent and Lang, 1982; Joshi et al., 2006). Simulations were performed considering the effect of terrain curvature. All simulations were implemented with a simulation time of 12 min (720 s). Table 2 reports the mass volume and values of the rheological parameters considered in the RAMMS::AVALANCHE simulations.

3.6. Validation

For each snow avalanche event, we compared the simulated flows computed by means of the two models with the observed geospatial data. The objective was to detect possible differences in the run-out distance (*r*), position, shape, depth (h_{max_dep}) and width (l_{max_dep}) of the observed and simulated deposit. The simulated deposits, maximum velocity, maximum flow height and maximum depth of the deposit computed by the two models were then compared to each other in order to find differences and similarities and evaluate the performance of each model. To statistically evaluate these differences, we selected two indices: (1) TSS (True Skill Statistic) and (2) D2PC (Distance To Perfect Classification). They are based on relations between true negative (TN), true positive (TP), false negative (FN) and false positive (FP) (Mcbride and Ebert, 2000). We chose those indices as they minimize the weight of TNs in the evaluation of simulations, since the amount of TN is usually the majority and can deviate the index outcome (Formetta et al., 2016). TSS is defined as the difference between the hit rate and false alarm rate (Eq. (6)). The index measures the ability of the model results to discern between non–snow avalanche and snow avalanche pixels. A large number of TN correspond to an overwhelmed false alarm value. If TN is large, the ratio between false positives and the sum of false positives and true negatives (FPR, Eq. (7)) tends to zero, and TSS tends to the between true positive and the sum of true positive and true negative (TPR, Eq. (8)) (Formetta et al., 2016).

$$TSS = \frac{(TP*TN) - (FP*FN)}{(TP + FN)*(FP + TN)} = TPR - FPR \tag{6}$$

where

$$FPR = \frac{FP}{FP + TN} \tag{7}$$

and

$$TPR = \frac{TP}{TP + FN} \tag{8}$$

TSS (Eq. (9)) ranges between −1 and 1, where the best value is 1. A TSS equal to 0 indicates an indiscriminate model, while a TSS equal to −1 indicates that the model results are no better than the results provided by a random model. The problem with TSS is that the hit rate and false alarm rate are treated equally, regardless of their possible consequences. D2PC measures the distance between the tested model point with the coordinates (FPR, TPR) and an ideal perfect point (0,1) within the plane (Formetta et al., 2016). This index ranges from 0 to 1, where 0 is the best match between simulation and observation.

$$D2PC = \sqrt{(1 - TPR)^2 + FPR^2} \tag{9}$$

To evaluate and discuss the simulation results also from a qualitative point of view, we defined two sets of ordinal variables to classify the simulation results based on the values of the statistical indexes. In particular, to define how well the simulation approximates the shape and position of the observed deposit, we segmented the D2PC range of value into four classes, while, to define the behaviour of the model in discerning snow avalanche and non-snow avalanche pixels, the range of values of TSS was segmented into five classes. Both D2PC and TSS classes are reported in Table 3.

Table 1
Snow mass volumes and rheological parameters tested in the FLO-2D simulations.

FLO–2D	Case study	
	"Knollgraben" avalanche	"Pichler Erschbaum" avalanche
Vol [m^3]	65,508	39,287
Cv [−]	0.45–0.70	0.45–0.70
γ_m [N m^{-3}]	3000	3000
τ_y [Pa]	500–3000	500–800
n–value [s $m^{-1/3}$]	0.50–0.30	0.20–0.45
η [Pa s]	0	0
K [−]	2000	2000

4. Results

4.1. FLO-2D simulations results

Two snow avalanches were modelled using the FLO–2D numerical model seeking the optimum condition of back-analysis. Table 4 reports the values of the rheological parameters employed in the simulations that better approximate the observed deposits of each case study and the peculiarities of the resulting simulated flows. The simulation of the Knollgraben snow avalanche well approximated the position and shape of the observed deposit, as shown by a D2PC value of 0.359. The released mass settled inside the channel of the Rio Lappago–Knollbach, along the entire length of the avalanche path. Nevertheless, most of the mass reached the observed deposition zone. The head of the deposit matched the observed runout distance by reaching the channel of the Rio Selva dei Molini–Mühlwalderbach. The maximum width of the simulated deposit (l_{max_dep}) was measured at the front of the deposit, and was equal to 88 m. The simulated deposit exceeded the width of the observed deposit, with snow settling inside the channel of the Rio Selva dei Molini–Mühlwalderbach, upstream of the confluence of

Table 2
Snow mass volumes and rheological parameters tested in the RAMMS::AVALANCHE simulations.

RAMMS::AVALANCHE		Case study	
		"Knollgraben" avalanche	"Pichler Erschbaum" avalanche
Vol [m^3]		65,508	39,287
ρ [kg m^{-3}]		300	300
N_0 [Pa]		0–2000	0–300
Rp [years]		30	10
Size		"*Large*"	"*Medium*"
μ [−]	Automatic method	0.170–0.290	0.20–0.39
	Variable method *(manually defined)*	–	0.250–0.350 (gully) 0.150–0.280 (alluvial fan and channel)
ξ [m s^{-2}]	Automatic method	1500–3500	1100–3250
	Variable method *(manually defined)*	–	1500–1800 (gully) 2500–3500 (alluvial fan and channel)

the two streams. The maximum height of the deposit (h_{max_dep}, Fig. 4B) was simulated within the channel, in correspondence to the alluvial fan. The simulated flow remained confined within the Rio Lappago – Knollbach (h_{max}, Fig. 4A), near the release area. The score of the TSS index was 0.428. The simulated maximum flow velocity was quite constant inside the gully and decreased when the mass reached the alluvial fan. The highest maximum flow velocity (V_{max} = 10.91 m/s) was simulated inside the gully (Fig. 4C).

The simulation of the Pichler Erschbaum snow avalanche well approximated the position of the observed deposit, as shown by a D2PC value equal to 0.243. Most of the released mass reached the observed deposition area and only a small amount settled inside the gully. As observed after the event, most of the simulated mass settled over the alluvial fan of the Rio di Monterosso–Rotenbergbach, with the front of the deposit reaching the channel of the Talvera–Talfer River. FLO-2D correctly simulated the main deposition of the simulated mass along the main flow direction and the separation of the flow into two branches at an altitude of around 1407 m a.s.l. However, the simulated mass flowed over the national road SS 508, depositing over the slope towards the channel of the Talvera–Talfer River. Furthermore, the simulated flow ran over the national road SS 508 towards south–west and deposited over it, widening the maximum width (l_{max_dep} = 141 m). As a consequence, less volume reached the area of the observed front of the deposit than that observed after the event, resulting in a deposit that covered less slope surfaces than the observed one. The maximum height of the deposit (h_{max_dep}, Fig. 4E) was simulated both at the apex of the alluvial fan and over the national road SS 508. The maximum flow depth (h_{max}, presented in Fig. 4D) was simulated inside the gully, immediately down-slope of the release area "Area 1". The score of the TSS index was equal to 0.659. The maximum simulated flow velocity was higher inside the gully, and it decreased when the mass reaches the alluvial fan. The highest maximum flow velocity (V_{max} = 12.13 m/s) was simulated inside the gully, immediately down-slope of the release area "Area 1" (Fig. 4F).

Table 3
Qualitative classifications of the statistical indices D2PC and TSS based on their value.

Range of values	D2PC qualitative classification	TSS qualitative classification
-1 ≤ x ≤ 0	–	The model behaves very badly in the simulation
0 < x ≤ 0.25	The simulation approximates very well the shape and position of the observed deposit	The model behaves badly in the simulation
0.25 < x ≤ 0.50	The simulation approximates well the shape and position of the observed deposit	The model behaves sufficiently well in the simulation
0.50 < x ≤ 0.75	The simulation partially approximates the shape and position of the observed deposit	The model behaves well in the simulation
0.75 < x ≤ 1	The simulation badly approximates the shape and position of the observed deposit	The model behaves very well in the simulation

Table 4
FLO–2D simulations that better approximate the observed deposit of each case study. For each simulation, the values of the rheological parameters and the features such as run-out distance (*r*), maximum flow velocity (V_{max}) and the flow depth (h_{max}), maximum height (h_{max_dep}) and width (l_{max_dep}) of the deposit and the score of the statistical indexes Distance to Perfect Classification (D2PC) and True Skill Statistics (TSS).

FLO–2D	Case study	
	"Knollgraben" avalanche	"Pichler Erschbaum" avalanche
Vol [m^3]	65,508	39,287
C_v [−]	0.55	0.55
γ_m [N m^{-3}]	3000	3000
τ_y [Pa]	2000	700
n – value [s $m^{-1/3}$]	0.25	0.40
η [Pa s]	0	0
K [−]	2000	2000
V_{max} [m/s]	10.90	12.13
h_{max_dep} [m]	5.10	3.20
h_{max} [m]	10.02	14.67
l_{max_dep} [m]	88.00	141
r [m]	2400	1480
D2PC [0 best value]	0.359	0.243
TSS [1 best value]	0.428	0.659

4.2. RAMMS::AVALANCHE simulations results

The investigated snow avalanche events were reproduced by use of the RAMMS::AVALANCHE numerical model. Table 5 reports the values of the rheological parameters employed in the simulations that better approximated the observed deposit of each case study and the peculiarities of the resulting simulated flows.

The simulation of the Knollgraben snow avalanche very well approximated the position and shape of the observed deposit, as shown by a D2PC value equal to 0.234. Most of the released mass reached the observed deposition area and settled inside the channel of the Rio Lappago–Knollbach. The front of the simulated deposit reached the channel of the Rio Selva dei Molini–Mühlwalderbach and the runout distance was comparable to the observed one. In contrast to the observed event, a small part of the simulated flow crossed the Rio Lappago–Knollbach and deposited in the alluvial fan, covering a surface of 1 ha. The absolute maximum width of the simulated deposit (85 m) corresponded to the maximum width of the secondary deposit, while the maximum width relative to the main deposit (l_{max_dep}) was measured at the front of the deposit, and was equal to 76 m. Maximum flow depth (h_{max}, Fig. 5A) was simulated inside the gully, upstream of the alluvial fan. The maximum height of the deposit (h_{max_dep}, Fig. 5B) was simulated within the channel on the alluvial fan. The model performed well in discerning snow avalanche and non-snow avalanche pixels, as shown by a TSS value equal to 0.671. The simulated maximum flow velocity was quite constant inside the gully and decreased when the mass reached the fan, as a consequence of slope reduction. The maximum flow velocity (V_{max} = 37.47 m/s) was simulated within the gully (Fig. 5C).

The simulation of the Pichler Erschbaum snow avalanche well approximated the position of the observed deposit, as shown by a D2PC value equal to 0.247. Most of the released mass reached the observed deposition area and settled over the alluvial fan of the Rio di Monterosso–Rotenbergbach. However, a large portion of the released snow mass accumulated at the end of the gully, where the slope gradient decreased and the alluvial fan began. The rest of the snow mass settled downwards from the fan apex and the front of the deposit reached the channel of the Talvera-Talfer River. As observed after the event, most of the mass of the simulated deposits elongated in the main flow direction. However, a small part of the

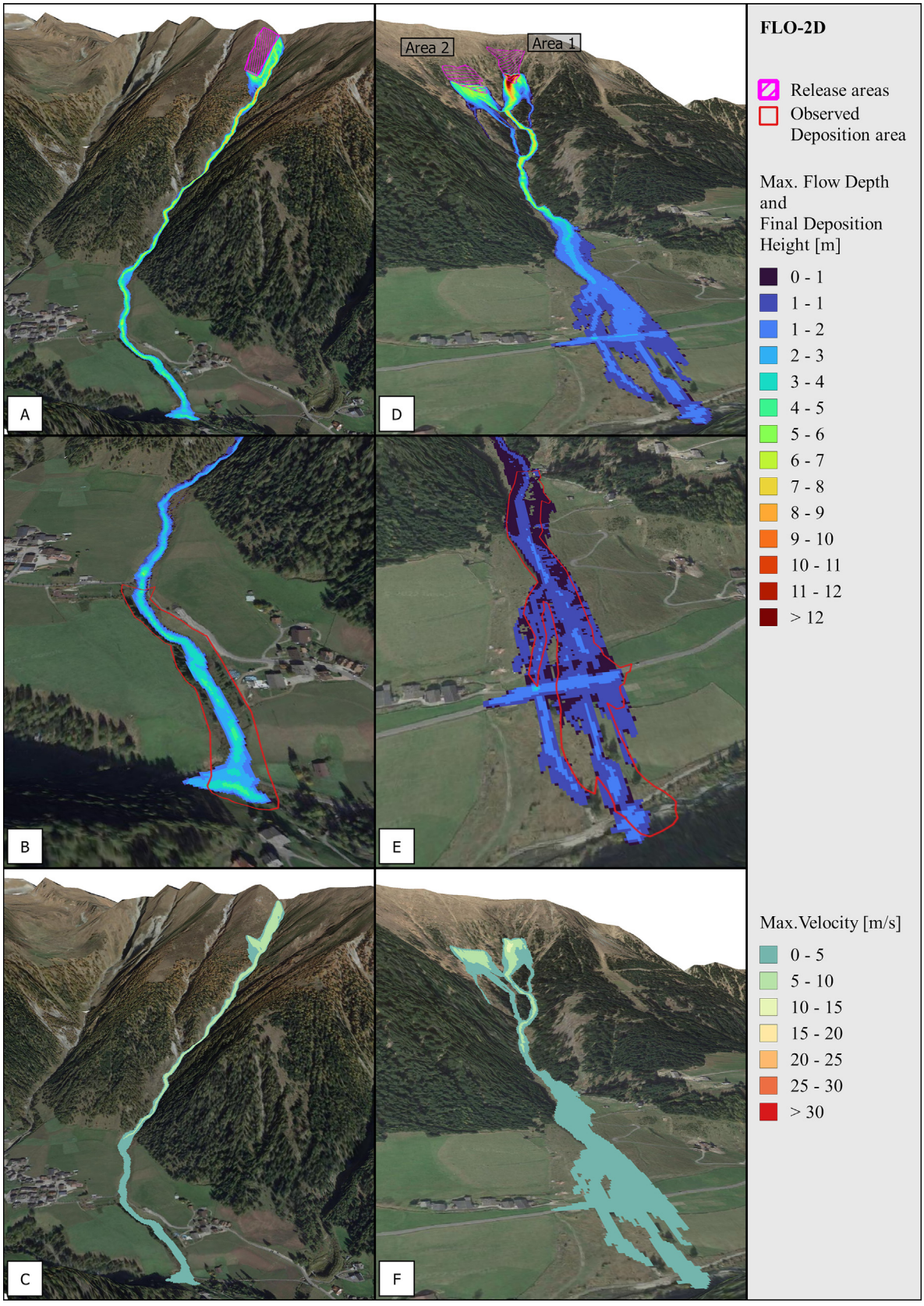

Fig. 4. Results of the FLO-2D simulations that better approximated the observed depositions of Knollgraben (left) and Pichler Erschbaum avalanches (right). The maximum flow depth (top), maximum deposition height (middle) and maximum flow velocity (bottom) of snow avalanches are represented together with their release areas and observed deposits.

Table 5
RAMMS::AVALANCHE simulations that better approximate the observed deposit of each case study. For each simulation, the values of the rheological parameters and the features such as runout distance (r), the maximum flow velocity (V_{max}) and the flow depth (h_{max}), maximum height (h_{max_dep}) and width (l_{max_dep}) of the deposit and the score of the statistical indexes Distance to Perfect Classification (D2PC) and True Skill Statistics (TSS).

RAMMS::AVALANCHE	Case study	
	"Knollgraben" avalanche	"Pichler Erschbaum" avalanche
Vol [m^3]	65,508	39,287
ρ [kg m^{-3}]	300	300
N_0 [Pa]	150	150
Rp [years]	30	/
Size	"Large"	/
μ [−]	Automatic Method 0.215–0.340	Manually defined 0.320 (gully) 0.180 (alluvial fan and channel)
ξ [m s^{-2}]	Automatic Method 1200–2250	Manually defined 1750 (gully) 3000 (alluvial fan and channel)
V_{max} [m/s]	37.47	34.26
h_{max_dep} [m]	6.43	2.91
h_{max} [m]	15.89	14.04
l_{max_dep} [m]	76.00	73.00
r [m]	2400	1480
D2PC [0 best value]	0.234	0.247
TSS [1 best value]	0.671	0.651

simulated flow spread over the alluvial fan and deposited on its left-hand side, covering a surface of 1.2 ha. This simulated deposit ran over a large section of a private road that serves some houses located on the left-hand side of the alluvial fan. The observed deposit only reached the most upstream switchback of the road. It resulted in a deposit that covered less surface than the one observed. The absolute maximum width of the simulated deposit (120 m) was measured in the upstream part of the alluvial fan, while the maximum width relative to the main deposit (l_{max_dep}) was measured over the state road SS 508 and was equal to 73 m. The maximum height of the deposit (h_{max_dep}, Fig. 5D) was simulated both at the apex of the alluvial fan and over the state road SS 508. The maximum flow depth (h_{max}, Fig. 5E) was simulated inside the gully, where the channel width was the narrowest. The score of the TSS index was equal to 0.651. The simulated flow velocity was at its maximum inside the gully in the headwater part (V_{max} = 34.26 m/s), to decrease when the mass reached the alluvial fan (Fig. 5F).

5. Discussion

We tested the performances of the simulation tools FLO-2D and RAMMS::AVALANCHE by back-calculating two well-documented snow avalanche events. For each case study, multiple simulations with both models were performed to find the combination of rheological parameters that better approximated the observed deposits. The results were then used to assess the performance of the model.

After calibration of the rheological parameters considered by the two models, the simulation results showed an overall good performance in reproducing the observed event. The values of frictional parameters μ and ξ (RAMMS::AVALANCHE) employed in the back–calculation of the Knollgraben snow avalanche are those automatically determined by the tool (Christen et al., 2017). These values resulted adequate during the back-calculation process, simplifying the calibration of the model to the definition of only one parameter (yield stress N_0). Adopting the frictional values computed by RAMMS::AVALANCHE for the Pichler Erschbaum snow avalanche, it was not possible to correctly reconstruct the observed deposit. After the calibration process, the values μ = 0.320 and ξ = 1750 m/s^2 for the gully area and μ = 0.180 and ξ = 3000 m/s^2 for the fan area were those that could better approximate the observed deposit. These values are in accordance with the range proposed by Christen et al. (2017) for "medium" size avalanches with a high return period (100 and 300 years). Regarding the simulations performed with FLO-2D, a more accurate calibration process was required due to the lack of reference values for the rheological parameters. Sediment concentration (C_v) resulted as being the parameter that most affected run-out distance. In all case studies, the sediment concentration value that better approximated the observed run-out distance was equal to 0.55. Therefore, it seems recommendable to adopt this value in future applications of this model for the simulation of snow avalanches. However, the use of FLO–2D on different events will give a useful hint about the choice of rheological parameters. Although the snow type was different in each case study, the RAMMS::AVALANCHE simulations that better reproduced the observed deposits employed the same snow cohesion value. (N_0 = 150 Pa). FLO-2D, instead, required different values of snow cohesion in each case study, with a higher yield stress (τ_y) value for the event characterised by wet snow (2000 Pa) compared to the dry snow event (700 Pa). Bartelt et al. (2015), Dent and Lang (1982) and Joshi et al. (2006) present a wide heterogeneity of snow cohesion values both for dry and especially for wet snow and it, therefore, results difficult to correctly assess these values. In our case, the snow cohesion values adopted in both models were within the ranges proposed by these studies. Furthermore, comparing the snow cohesion values used with both models and for all other rheological parameters seemed to be pointless since the frictional dissipation equations implemented in the two models were very different.

By comparing the results of the simulations performed with both models and the related statistical indices scores, it is possible to highlight the differences between them and the relative advantages or drawbacks. With both FLO–2D and RAMMS::AVALANCHE it was possible to approximate well the observed deposits of each event (Table 3). Based on the scores of the statistical indexes D2PC and TSS, both models very well approximated the observed deposit of the Pichler Erschbaum snow avalanche, scoring almost identical D2PC and TSS values. For the Knollgraben snow avalanche case study, instead, RAMMS::AVALANCHE performed better than FLO-2D in approximating the observed deposits, both in shape and position, as shown by the value of the two statistical indexes (Tables 4 and 5). It is important to note that statistical indices alone may not accurately reflect the performance of the model and that a critical visual examination should be included in the evaluation of the results. The deposits simulated by the models for the Pichler Erschbaum case study, despite having identical D2PC and TSS scores, had very different shapes. FLO–2D (D2PC = 0.243; TSS = 0.653) simulated a flow very sensitive to the presence of the national road SS 508. Therefore, the head of the simulated deposit divided into different branches downwards of the state road. RAMMS::AVALANCHE (D2PC = 0.247; TSS = 0.651), instead, simulated a more compact deposit, better approximating the shape of the observed head of the deposit. RAMMS::AVALANCHE simulated the snow deposition on the left-hand side of the alluvial fan and at the apex of the alluvial fan that was not observed after the event. For the Knollegaben snow avalanche, FLO–2D (D2PC = 0.359; TSS = 0.428) simulated the deposition of material along the entire path of the avalanche. As a consequence, because of the reduced mass that reached the observed deposition area, the simulated deposit filled only the lower part of the channel cross-section, while the observed deposit reached almost the top of the channel banks. RAMMS::AVALANCHE (D2PC = 0.234; TSS = 0.671) simulated less deposition inside the gully and more mass reaching the observed deposition area, more filling the cross-section of the channel. Despite that, the model simulated the overflow and consequent deposition of snow on the right-hand side of the alluvial fan. Assessing the performance of the models in simulating the maximum deposit height (h_{max_dep}) results are more complicated since the position where the maximum deposit height was observed is not specified in the post-event survey reports. However, it is possible to highlight that, for the same case study, both models underestimated the observed h_{max_dep} (underestimation up to 4 m) and the values were different (up to 1 m). Furthermore, both models simulated h_{max_dep} in different positions.

Taking into account the maximum flow velocities (V_{max}), RAMMS::AVALANCHE simulated flows with V_{max} two- to three times higher than FLO-2D. This remarkable difference is particularly evident immediately

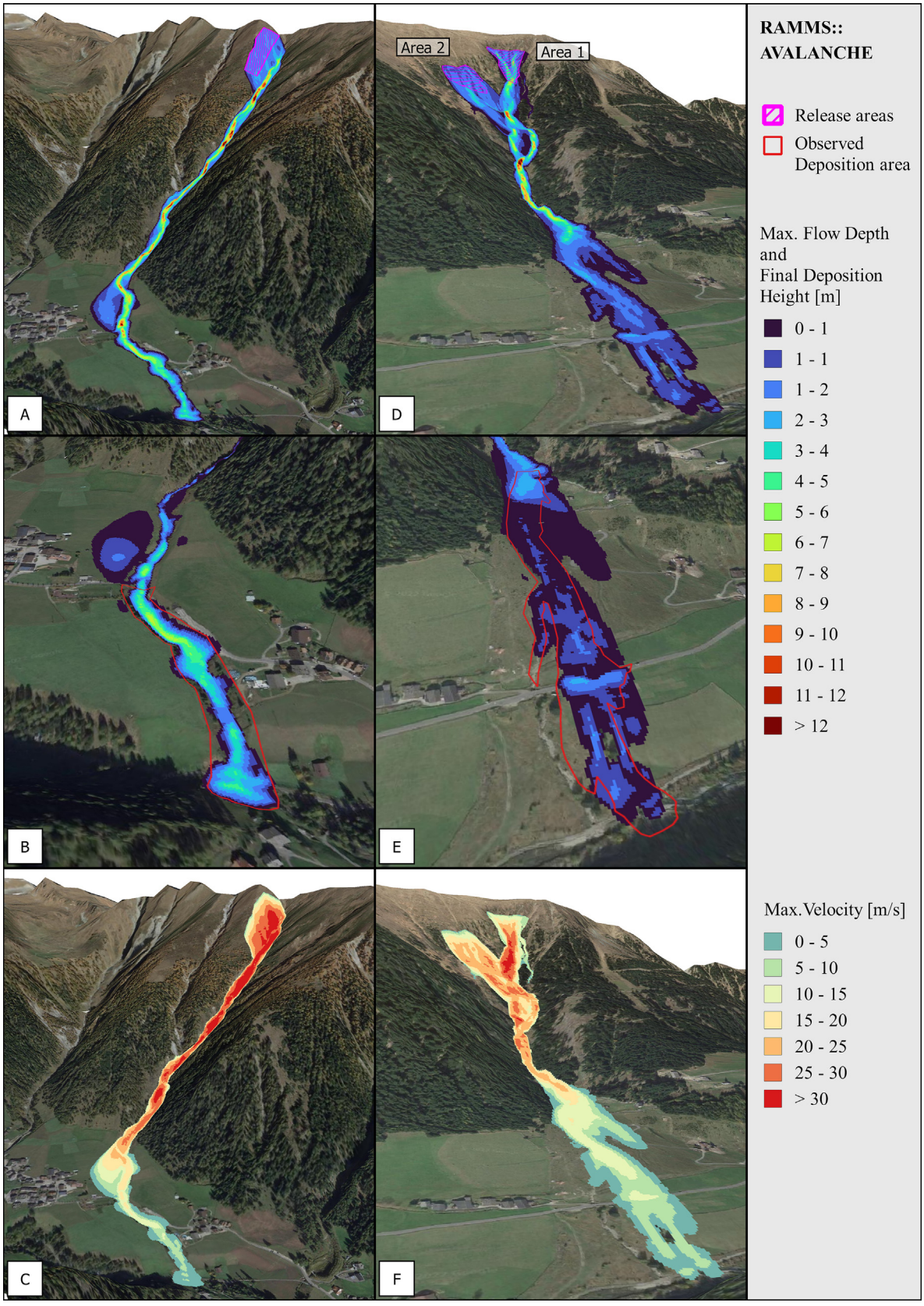

Fig. 5. Results of the RAMMS::AVALANCHE simulations that better approximated the observed depositions of the Knollgraben (left) and Pichler Erschbaum avalanches (right). The maximum flow depth (top), maximum deposition height (middle) and maximum flow velocity (bottom) are represented together with their release areas and observed deposits.

downstream of the release areas and inside the gullies. The maximum flow velocities simulated by the RAMMS::AVALANCHE for the dry snow avalanche were consistent with the values proposed in the literature (Havens et al., 2014; Kogelnig et al., 2011; Lacroix et al., 2012; Rudolf-Miklau et al., 2015; Košová et al., 2022; Vilajosana et al., 2007; Vriend et al., 2013), while V_{max} of the wet snow avalanche results high compared to the proposed range of values, resembling those for dry avalanches. The V_{max} values simulated by FLO–2D for wet snow avalanches were quite low, but within the ranges reported in the literature. However, the V_{max} simulated for the dry snow avalanche was too low and not comparable with the values in the literature. The difference in maximum velocity simulated by the two models was more pronounced within the channels upstream of the alluvial fans. In these areas, RAMMS::AVALANCHE simulated velocities of 20 up to 30 m/s higher than FLO-2D for the Knollgraben avalanche (max difference equals 36 m/s) and of 15 up to 25 m/s for the Pichler Erschbaum avalanche (max difference equals 31 m/s). The velocity difference decreased once the flow reached the alluvial fan, still remaining non-negligible (up to 15 m/s in both case studies). In the case of the Pichler Erschbauml avalanche, the flow simulated by RAMMS::AVALANCHE arrived at the deposition area with a greater velocity difference (up to 10 m/s) than in the Knollgraben avalanche, where the avalanche front simulated by RAMMS::AVALANCHE arrived in the Selva dei Molini-Mühlwalderbach stream even with lower velocity than in FLO-2D (up to 2.5 m/s less). Although RAMMS::AVALANCHE generally better approximated the shape and position of the observed deposits, it should also be considered that due to the high flow momentum, phenomena of channel overflow may be produced, especially where there are abrupt changes in topography. In both study cases, the model simulated the deposition of snow where it was not observed. This may not be a problem when back–calculating observed events; however, it may result in an overestimation of the area affected by snow avalanches and of flow velocities and pressures during hazard and risk assessment procedures. The results were less accurate in the approximation of the shapes of the observed deposits, and the low maximum velocities simulated may not be adequate for the calculation of the impact pressures. The high uncertainty of the velocities simulated by the models affects hazard mapping, providing results that can overestimate or underestimate actual velocities. Considering low velocities could lead to underestimation of dynamic hazard. In contrast, considering high speed values could lead to exaggerating the size of protection measures. The joint use of results from two models could be an effective method to better calibrate the design of protection works.

The results produced by FLO-2D are encouraging, also considering the lack of implementation for snow avalanches and the absence of references for the calibration of rheological parameters (Barbolini and Savi, 2014; Moro, 2009). Future applications of FLO–2D for snow avalanche events are necessary to improve the choice of the model friction parameters and, consequently, contribute to their use in modelling snow avalanches and risk and hazard assessment.

6. Conclusions

This study investigated the performances of the two-dimensional numerical simulation models FLO-2D and RAMMS::AVALANCHES in back-calculating snow avalanche deposition areas. Although FLO-2D was developed to simulate floods (also associated with bed load transport) and events of debris flow/flood, we attempted to evaluate its use for snow avalanches. We performed the back-analysis of two well-documented avalanches in the autonomous province of Bolzano-Bozen (IT): a dry and a wet snow avalanche. The strength and limitations of both models were evaluated by comparing the model results with the observed deposition areas, adopting statistical indices (TSS and D2PC).

RAMMS::AVALANCHE generally well approximated the observed deposits, showing good TSS and D2PC values. The maximum flow velocities simulated by RAMMS::AVALANCHE produced values in the order of 30–40 m/s for both types of snow. Although the simulated velocities for the dry snow avalanche were consistent with the values proposed in the literature, the values for wet snow avalanches were too high. The high velocities and the associated channel overflows simulated by RAMMS::AVALANCHE provided in both case studies precautionary results from the perspective of hazard mapping. FLO-2D results were less accurate in reproducing the observed deposits, showing less suitable TSS and D2PC values compared to the RAMMS::AVALANCHE simulations. The maximum flow velocities simulated by the model were in some cases excessively low (order of 10–12 m/s), especially for dry snow avalanches. Since the rheological parameters considered by FLO-2D are not those typical of a snow avalanche rheology, an effective calibration of these parameters was obtained after a meticulous and accurate iterative process due to the lack of comparable implementations (absence of references for the rheological parameters). In particular, the results of the model were very sensitive to the sediment concentration (C_v) of the fluid and, to a lesser extent, to the yield stress (τ_y) and Manning coefficient (n) attributed to the slope of the avalanche site. In particular, the flow resistance equation of the model was adapted to a form more similar to the VSG model by omitting the dynamic viscosity coefficient. Further investigation on the employment of this coefficient also for simulating snow avalanches could be carried out to better refine this choice. Despite that, the results produced by FLO-2D are encouraging. They proved to have good potential to reproduce the motion of snow avalanches and they added reference values for practitioners, which often demand a straightforward and low time-consuming implementation of the models.

For a robust and reliable use of FLO-2D for avalanche simulation and related hazard mapping, more studies based on back-analysis of snow avalanche events are necessary to define adequate reference values of the rheological parameters for different types of snow avalanches.

It is also worth concluding that the results of different simulation models should be jointly considered so that a greater number of possible modelling scenarios can be accounted for the production of snow avalanche hazard and risk maps. In this way, a much more cautionary implementation of mitigation structures could be achieved, being aware of the possible occurrence of snow avalanches with different features in the same catchment.

CRediT authorship contribution statement

Marco Martini: Conceptualization, Methodology, Validation, Investigation, Writing - Original Draft.

Tommaso Baggio: Conceptualization, Methodology, Validation, Writing – Review and Editing, Supervision.

Vincenzo D'Agostino: Conceptualization, Review and Editing, Supervision.

Data availability

The authors do not have permission to share data.

Declaration of competing interest

The authors declare that they have no known competing financial interests or personal relationships that could have appeared to influence the work reported in this paper.

Acknowledgements

The research was supported by the funds of the University of Padova (Italy): BIRD-DOR 2022, Prof. Vincenzo D'Agostino. Authors wish to thank the Snow Avalanche Cadastre of the Civil Protection Agency of the Autonomous Province of Bolzano (IT) for the post-event data and the two anonymous reviewers for their useful suggestions and comments.

References

Aaron, J., Conlan, M., Johnston, K., Gauthier, D., Mcdougall, S., 2016. Adapting and calibrating the DAN3D dynamic model for North American snow avalanche runout modelling. International Snow Science Workshop, Breckenridge, Colorado, 2016, pp. 825–829.

Adler, S., Chimani, B., Drechsel, S., Haslinger, K., Hiebl, J., Meyer, V., Resch, G., Rudolph, J., Vergeiner, J., Zingerle, C., 2015. Il clima del Tirolo-Alto Adige-Bellunese. Zentralanstalt fur Meteorologie und Geodynamik, Ripartizione Protezione antincendi e civile–Provincia Autonoma di Bolzano, Agenzia Regionale per la Prevenzione e Protezione Ambientale del Veneto, Padova, pp. 31–38.

Ancey, C., 2008. Snow avalanches. Geomorphological Fluid Mechanics: Selected Topics in Geological and Geomorphological Fluid Mechanics, pp. 319–338 https://doi.org/10.1007/3–540-45670-8_13.

Barbolini, M., Savi, F., 2014. Snow avalanche dynamics simulation and hazard mapping using FLO-2D. Conference: Interpraevent 2008, Dorbrin, Austria, pp. 26–27 https://doi.org/10.13140/2.1.3166.6249.

Barbolini, M., Gruber, U., Keylock, C.J., Naaim, M., Savi, F., 2000. Application of statistical and hydraulic-continuum dense-snow avalanche models to five real European sites. Cold Reg. Sci. Technol. 31, 133–149. https://doi.org/10.1016/S0165-232X(00)00008-2.

Bartelt, P., Valero, C.V., Feistl, T., Christen, M., Bühler, Y., Buser, O., 2015. Modelling cohesion in snow avalanche flow. J. Glaciol. 61, 837–850. https://doi.org/10.3189/2015JoG14J126.

Bartelt, P., Buser, O., Vera Valero, C., Bühler, Y., 2016. Configurational energy and the formation of mixed flowing/powder snow and ice avalanches. Ann. Glaciol. 57, 179–188. https://doi.org/10.3189/2016aog71a464.

Blagovechshenskiy, V., Medeu, A., Gulyayeva, T., Zhdanov, V., Ranova, S., Kamalbekova, A., Aldabergen, U., 2023. Application of artificial intelligence in the assessment and forecast of avalanche danger in the Ile Alatau ridge. Water (Switzerland) 15. https://doi.org/10.3390/w15071438.

Buser, O., Bartelt, P., 2009. Production and decay of random kinetic energy in granular snow avalanches. J. Glaciol. 55, 3–12. https://doi.org/10.3189/002214309788608859.

Choubin, B., Borji, M., Mosavi, A., Sajedi-Hosseini, F., Singh, V.P., Shamshirband, S., 2019. Snow avalanche hazard prediction using machine learning methods. J. Hydrol. (Amst) 577. https://doi.org/10.1016/j.jhydrol.2019.123929.

Choubin, B., Borji, M., Hosseini, F.S., Mosavi, A., Dineva, A.A., 2020. Mass wasting susceptibility assessment of snow avalanches using machine learning models. Sci. Rep. 10. https://doi.org/10.1038/s41598-020-75476-w.

Christen, M., Bartelt, P., Kowalski, J., 2010a. Back calculation of the In den Arelen avalanche with RAMMS: interpretation of model results. Ann. Glaciol. 51, 161–168. https://doi.org/10.3189/172756410791386553.

Christen, M., Kowalski, J., Bartelt, P., 2010b. RAMMS: numerical simulation of dense snow avalanches in three-dimensional terrain. Cold Reg. Sci. Technol. 63, 1–14. https://doi.org/10.1016/j.coldregions.2010.04.005.

Christen, M., Bartelt, P., Bühler, Y., Deubelbeiss, Y., Salz, M., Schneider, M., Schumacher, L., 2017. RAMMS::AVALANCHE User Manual v1.7.0 104.

Civil Protection Agency of the autonomous province of Bolzano–Bozen - Provincial Functional Centre, 2017. Leistungskatalog für die Erstellung des Gefahrenzonenplanes Prozess Lawinen (Bozen - Bolzano).

Dent, J.D., Lang, T.E., 1982. Experiments on mechanics of flowing snow. Cold Reg. Sci. Technol. 5, 253–258. https://doi.org/10.1016/0165-232X(82)90018-0.

Dreier, L., Bühler, Y., Ginzler, C., Bartelt, P., 2016. Comparison of simulated powder snow avalanches with photogrammetric measurements. Ann. Glaciol. 57, 371–381. https://doi.org/10.3189/2016AoG71A532.

Eckert, N., Giacona, F., 2023. Towards a holistic paradigm for long-term snow avalanche risk assessment and mitigation. Ambio 52, 711–732. https://doi.org/10.1007/s13280-022-01804-1.

Eckert, N., Parent, E., Richard, D., 2007. Revisiting statistical-topographical methods for avalanche predetermination: Bayesian modelling for runout distance predictive distribution. Cold Reg. Sci. Technol. 49, 88–107. https://doi.org/10.1016/j.coldregions.2007.01.005.

Eckert, N., Parent, E., Naaim, M., Richard, D., 2008. Bayesian stochastic modelling for avalanche predetermination: from a general system framework to return period computations. Stoch. Env. Res. Risk A. 22, 185–206. https://doi.org/10.1007/s00477-007-0107-4.

Fischer, J.T., Fromm, R., Gauer, P., Sovilla, B., 2014. Evaluation of probabilistic snow avalanche simulation ensembles with Doppler radar observations. Cold Reg. Sci. Technol. 97, 151–158. https://doi.org/10.1016/j.coldregions.2013.09.011.

FLO-2D, 2019. FLO-2D Reference Manual.

Formetta, G., Capparelli, G., Versace, P., 2016. Evaluating performance of simplified physically based models for shallow landslide susceptibility. Hydrol. Earth Syst. Sci. 20, 4585–4603. https://doi.org/10.5194/hess-20-4585-2016.

Gauer, P., 2014. Comparison of avalanche front velocity measurements and implications for avalanche models. Cold Reg. Sci. Technol. 97, 132–150. https://doi.org/10.1016/j.coldregions.2013.09.010.

Gruber, U., Margreth, S., 2001. Winter 1999: a valuable test of the avalanche-hazard mapping procedure in Switzerland. Ann. Glaciol. 32, 328–332. https://doi.org/10.3189/172756401781819238.

Gubler, H., 1994. Swiss avalanche-dynamics procedures for dense flow avalanches. Eidg. Institut für Schnee- und Lawinenforschung, Weissfluhjoch/Davos, Switzerland Mitteilung No. 51 8 pp.

Harbitz, C., Issler, D., Keylock, C., 1998. Conclusions from a Recent Survey of Avalanche Computational Models. Publikasjon - Norges Geotekniske Institutt, pp. 128–135.

Havens, S., Marshall, H.-P., Johnson, J.B., Nicholson, B., 2014. Calculating the velocity of a fast-moving snow avalanche using an infrasound array. Geophys. Res. Lett. 41, 6191–6198. https://doi.org/10.1002/2014GL061254.

Jamieson, B., Margreth, S., Jones, A., 2008. Application and limitations of dynamic models for snow avalanche hazard mapping. International Snow Science Workshop Proceedings 2008, pp. 730–739.

Janeras, M., Oller, P., Arancibia, R., Pons, J., Costa, O., Asensio, D., 2013. Back-analysis modelling of the catastrophic avalanches in Sewell, Central Chilean Andes. International Snow Science Workshop Grenoble – Chamonix Mont-Blanc.

Joshi, S.K., Mahajan, P., Upadhyay, A., 2006. Study of layered snow under shear and tension. International Snow Science Workshop.

Kogelnig, A., Suriñach, E., Vilajosana, I., Hübl, J., Sovilla, B., Hiller, M., Dufour, F., 2011. On the complementariness of infrasound and seismic sensors for monitoring snow avalanches. Nat. Hazards Earth Syst. Sci. 11, 2355–2370. https://doi.org/10.5194/NHESS-11-2355-2011.

Košová, V., Molokáč, M., Čech, V., Jesenský, M., 2022. Avalanche hazard modelling within the Král'ova Hol'a area in the low Tatra Mountains in Slovakia. Land (Basel) 11. https://doi.org/10.3390/land11060766.

Lacroix, P., Grasso, J.-R., Roulle, J., Giraud, G., Goetz, D., Morin, S., Helmstetter, A., Lacroix, C., 2012. Monitoring of snow avalanches using a seismic array: location, speed estimation, and relationships to meteorological variables. J. Geophys. Res. 117, 1034. https://doi.org/10.1029/2011JF002106.

Lied, K., Bakkehoi, S., 1981. Empirical calculations of snow-avalanche run-out distance based on topographic parameters. Publikasjon - Norges Geotekniske Institutt 165–177. https://doi.org/10.3189/s0022143000010704.

Liu, Y., Chen, X., Yang, J., Li, L., Wang, T., 2023. Snow avalanche susceptibility mapping from tree-based machine learning approaches in ungauged or poorly-gauged regions. Catena (Amst) 224. https://doi.org/10.1016/j.catena.2023.106997.

Maggioni, M., Freppaz, M., Christen, M., Bartelt, P., Zanini, E., 2012. Back-calculation of small avalanche with the 2D avalanche dynamics model RAMMS : four events artificially triggered at the Seehore test site in Aosta Valley (NW-Italy). Proceedings 2012 International Snow Science Workshop.

Mcbride, J.L., Ebert, E.E., 2000. Verification of quantitative precipitation forecasts from operational numerical weather prediction models over Australia. Weather Forecast. 15, 103–121. https://doi.org/10.1175/1520-0434(2000)015<0103:VOQPFF>2.0.CO;2.

McClung, D.M., 2001. Extreme avalanche runout: a comparison of empirical models. Can. Geotech. J. 38, 1254–1265. https://doi.org/10.1139/t01-041.

McClung, D., Schaerer, P.A., 2006. The Avalanche Handbook. The Mountaineers Books.

Mergili, M., Fischer, J.T., Krenn, J., Pudasaini, S.P., 2017. R.avaflow v1, an advanced open-source computational framework for the propagation and interaction of two-phase mass flows. Geosci. Model Dev. 10, 553–569. https://doi.org/10.5194/gmd-10-553-2017.

Meunier, M., Ancey, C., 2004. Towards a conceptual approach to predetermining long-return-period avalanche run-out distances. J. Glaciol. 50, 268–278. https://doi.org/10.3189/172756504781830178.

Moro, F., 2009. Snow Avalanches: Hazard Maps and Passive Defence Structures. PhD Thesis. Dipartimento di Geoscienze, Università degli Studi di Padova.

Naaim, M., Faug, T., Naaim-Bouvet, F., 2003. Dry granular flow modelling including erosion and deposition. Surv. Geophys. https://doi.org/10.1023/B:GEOP.0000006083.47240.4c.

Naaim, M., Durand, Y., Eckert, N., Chambon, G., 2013. Dense avalanche friction coefficients: influence of physical properties of snow. J. Glaciol. 59, 771–782. https://doi.org/10.3189/2013JoG12J205.

O'Brien, J.S., Julien, P.Y., Fullerton, W.T., 1993. Two-dimensional water flood and mudflow simulation. J. Hydraul. Eng. 119 (2), 244–261. https://doi.org/10.1061/(asce)0733-9429(1993)119:2(244).

Perla, R., Cheng, T.T., Mcclung, D.M.M., By, R., Mcclung, D.M.M., 1980. A two-parameter model of snow-avalanche motion. J. Glaciol. 26, 197–207. https://doi.org/10.3189/S002214300001073X.

Pistocchi, A., Notarnicola, C., 2013. Data-driven mapping of avalanche release areas: a case study in South Tyrol, Italy. Nat. Hazards 65, 1313–1330. https://doi.org/10.1007/s11069-012-0410-3.

Riba Porras, S., García-Sellés, C., Bartelt, P., Stoffel, L., 2018. Analysis of one avalanche zone in the eastern Pyrenees (Val d'Aran) using historical analysis, snow-climate data and mixed flowing/powder avalanche modelling. Proceedings, International Snow Science Workshop, Innsbruck, Austria.

Rudolf-Miklau, F., Sauermoser, S., Mears, A.I., 2015. The Technical Avalanche Protection Handbook, The Technical Avalanche Protection Handbook. Wiley Blackwell https://doi.org/10.1002/9783433603840.

Salm, B., 1966. Contribution to avalanche dynamics. International Association of Scientific Hydrology, Publication 69 (Symposium at Davos 1965–Scientific Aspects of Snow and Ice Avalanches).

Salm, B., 1993. Flow, flow transition and runout distances of flowing avalanches. Ann. Glaciol. 18, 221–226. https://doi.org/10.1017/s0260305500011551.

Salm, B., 2004. A short and personal history of snow avalanche dynamics. Cold Reg. Sci. Technol. 39, 83–92. https://doi.org/10.1016/j.coldregions.2004.06.004.

Salm, B., Burkard, A., Gubler, H.U., 1990. Berechnung von Fliesslawinen: eine Anleitung für Praktiker mit Beispielen. Eidgenössisches Institut für Schnee-und Lawinenforschung, Weissfluhjoch/Davos.

Sampl, P., Zwinger, T., 2004. Avalanche simulation with SAMOS. Ann. Glaciol. 38, 393–398. https://doi.org/10.3189/172756404781814780.

Sanz-Ramos, M., Andrade, C.A., Oller, P., Furdada, G., Bladé, E., Martínez-Gomariz, E., 2021. Reconstructing the snow avalanche of Coll de Pal 2018 (SE Pyrenees). GeoHazards 2, 196–211. https://doi.org/10.3390/geohazards2030011.

Savage, S.B., Hutter, K., 1989. The motion of a finite mass of granular material down a rough incline. J. Fluid Mech. 199, 177–215. https://doi.org/10.1017/S0022112089000340.

Savage, S.B., Hutter, K., 1991. The dynamics of avalanches of granular materials from initiation to runout. Part I: analysis. Acta Mech. 86, 201–223. https://doi.org/10.1007/BF01175958.

Schmidtner, K., Bartelt, P., Fischer, J., Sailer, R., Granig, M., 2018. Comparison of Powder Snow Avalanche Simulation Models (RAMMS and SamosAT) Based on Reference Events in Switzerland.

Schweizer, J., Jamieson, J.B., Schneebeli, M., 2003. Snow avalanche formation. Rev. Geophys. 41 (4). https://doi.org/10.1029/2002RG000123.

Singh, D.K., Mishra, V.D., Gusain, H.S., 2020. Simulation and analysis of a snow avalanche accident in lower Western Himalaya, India. J. Indian Soc. Remote Sens. 48, 1555–1565. https://doi.org/10.1007/s12524-020-01178-5.

Sovilla, B., Burlando, P., Bartelt, P., 2006. Field experiments and numerical modelling of mass entrainment in snow avalanches. J. Geophys. Res. Earth Surf. 111, 3007. https://doi.org/10.1029/2005JF000391.

Sovilla, B., Schaer, M., Kern, M., Bartelt, P., 2008. Impact pressures and flow regimes in dense snow avalanches observed at the Vallée de la Sionne test site. J. Geophys. Res. Earth Surf. 113, 1010. https://doi.org/10.1029/2006JF000688.

Toft, H.B., Müller, K., Hendrikx, J., Jaedicke, C., Bühler, Y., 2023. Can big data and random forests improve avalanche runout estimation compared to simple linear regression? Cold Reg. Sci. Technol. 211. https://doi.org/10.1016/j.coldregions.2023.103844.

Valt, M., Cianfarra, P., 2021. L'Inverno 2020–2021 sulle Alpi Italiane. Neve e Valanghe Speciale S. pp. 9–19.

Vilajosana, I., Khazaradze, G., Suriñach, E., Lied, E., Kristensen, K., 2007. Snow avalanche speed determination using seismic methods. Cold Reg. Sci. Technol. 49, 2–10. https://doi.org/10.1016/J.COLDREGIONS.2006.09.007.

Voellmy, A., 1955. Über die Zerstörungskraft von Lawinen. Schweizerische Bauzeitung 73, 159–165.

Vriend, N.M., McElwaine, J.N., Sovilla, B., Keylock, C.J., Ash, M., Brennan, P., 2013. High-resolution radar measurements of snow avalanches. Geophys. Res. Lett. 40, 727–731. https://doi.org/10.1002/GRL.50134.

Woolhiser, D.A., 1975. Simulation of unsteady overland flow. Unsteady Flow in Open Channels.

Zugliani, D., Rosatti, G., 2021. TRENT2D□: an accurate numerical approach to the simulation of two-dimensional dense snow avalanches in global coordinate systems. Cold Reg. Sci. Technol. 190, 103343. https://doi.org/10.1016/j.coldregions.2021.103343.